nature neuroscience

ARTICLES

https://doi.org/10.1038/s41593-019-0440-1

Parietal neurons encode information sampling based on decision uncertainty

Mattias Horan[1], Nabil Daddaoua[1,2] and Jacqueline Gottlieb[1,2,3*]

During natural behavior, animals actively gather information that is relevant for learning or actions; however, the mechanisms of active sampling are rarely investigated. We tested parietal neurons involved in oculomotor control in a task in which monkeys made saccades to gather visual information relevant to a subsequent action. We show that the neurons encode, before the saccade, the information gain (reduction in decision uncertainty) that the saccade was expected to bring for the following action. Sensitivity to information gain correlates with the monkeys' efficiency at processing the information in the post-saccadic fixation, but is independent of neuronal reward sensitivity. Reward sensitivity, in turn, is unreliable across task contexts, inconsistent with the view that the cells encode economic utility. The findings suggest that parietal cells involved in oculomotor decisions show uncertainty-dependent boosts of neural gain that facilitate the implementation of active sampling policies, including the selection of relevant cues and the efficient use of the information delivered by these cues.

To survive and thrive in complex environments, animals must make decisions under uncertainty and gather information that reduces that uncertainty. In neuroscience and psychology, information accumulation is studied by presenting participants with given (experimenter-selected) sensory cues and asking them to make decisions based on those cues[1]. In natural behavior, however, animals use active sensing strategies, whereby they endogenously decide what information to sample: which stimuli to listen, touch or look at to guide future actions. However, the neural mechanisms of these strategies are seldom investigated[2–4].

In humans and monkeys, the primary means of sampling visual information are rapid eye movements (saccades) that place the fovea on selected items in visual scenes. Cortical neurons involved in spatial attention and saccadic decisions have spatial receptive fields (RFs) and selectively encode attention-worthy stimuli and locations[5,6], but the significance of these selective responses has been intensely debated. A long-standing question, debated primarily in the lateral intraparietal area (LIP), is whether saccade-related responses encode attentional priority or the reward values of alternative actions[4,7].

We have argued that understanding this question requires the use of behavioral tasks in which participants deploy eye movements not merely to gather rewards, as has been the prevailing practice so far, but also to serve their natural role of gathering information[2–4]. To this end, we trained monkeys on a new task in which they made two coordinated saccades: an initial saccade to gather information from a visual cue and a subsequent saccade to report a decision based on the information. In an initial study[8] using this paradigm, we showed that pre-saccadic responses of LIP cells encoded the percentage validity of alternative cues—that is, the extent to which a cue, when examined during the post-saccadic fixation, will reduce the uncertainty of the subsequent action.

Here, we show that LIP neurons also encode expected information gain (IG) based on dynamic changes in decision uncertainty. The neurons had stronger pre-saccadic responses if the monkeys had ex ante decision uncertainty and expected the initial saccade to reduce that uncertainty compared with an alternative context in which the monkeys had prior knowledge of the appropriate final action and expected the saccade merely to bring redundant information. Moreover, the neural sensitivity to IG was not correlated with the sensitivity to reward gain, and reward sensitivity showed positive or negative scaling in different task contexts, inconsistent with the idea that the cells encode the economic utility. Instead, the findings support a two-stage model of attention control[9]. A monitoring stage that seems to be implemented outside LIP allocates control based on the utility (costs and benefits) of alternative actions, and a regulatory stage, which includes the parietal cortex, implements the required control, in part through an uncertainty-dependent enhancement of neural gain that enables animals to select informative cues and efficiently process the information conveyed by these cues.

Results

Two monkeys (*Macaca mulatta*) performed an information-sampling task in which they made two coordinated saccades on each trial (Fig. 1a). The monkeys made their first saccade to a cue to obtain visual information (100% coherent motion signaling the correct decision alternative) and a second saccade to indicate the final decision based on the information (a saccade to one of the alternatives).

We varied the IGs of the initial saccade through blockwise manipulations of the ex ante uncertainty about the correct final action. In informative (INF) trial blocks, the monkeys started each trial with uncertainty about their final decision and could expect that the motion will resolve their uncertainty (indicating which alternative was correct on that trial; Fig. 1a, top). In contrast, in uninformative (unINF) blocks, the correct target was fixed across trials so that the monkeys could identify the correct second saccade in advance and the motion merely confirmed their prior expectations (Fig. 1a, bottom). The INF and unINF conditions were presented in alternating blocks of 50 correct trials, with the initial block type randomized across sessions (Fig. 1b).

Importantly, the monkeys had to make their first saccade to the cue in both the INF and unINF blocks, meaning that this saccade

[1]Department of Neuroscience, Columbia University, New York, NY, USA. [2]Zuckerman Mind Brain Behavior Institute, Columbia University, New York, NY, USA. [3]The Kavli Institute for Brain Science, Columbia University, New York, NY, USA. *e-mail: jg2141@columbia.edu

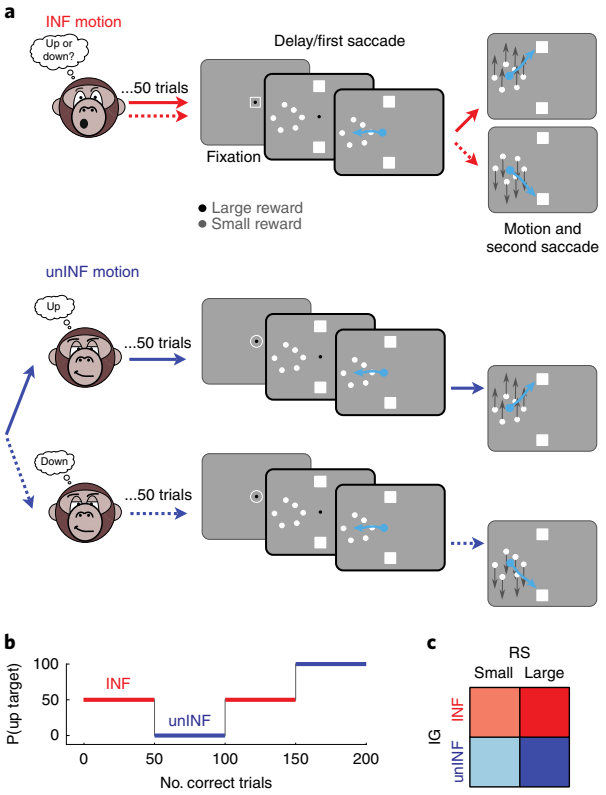

Fig. 1 | Task design. a, Trial structure. All the trials had an identical structure and differed only in whether they appeared in INF or unINF blocks. Each trial started with a fixation stage when the monkeys were informed about the RS (large or small, 300 ms versus 100 ms solenoid open time) through the fixation point color and the block type (INF or unINF) through an openframe shape around the fixation point. This was followed by the onset of the trial display, containing two targets (white squares) and a cue (a patch of small stationary dots). After viewing the display for 500 ms during central fixation (delay period), the fixation point disappeared, instructing the monkey to make the first saccade to the cue. When the monkey fixated on the cue for 100 ms, the dots began to move with 100% coherence toward one of the targets (motion and second saccade, gray arrows). The monkey was free to make its final decision and received a reward if it made a second saccade (cyan arrow) to the target that had been cued by the motion. The dark frames highlighting the delay and first saccade periods indicate the epochs of interest for the neural data analysis. unINF blocks (lower two rows) had an identical trial structure but were distinguished from INF blocks by the distribution of the correct second saccade targets. In INF blocks, the correct target (in this example, up or down, indicated by the solid and broken red arrows) was randomly selected on each trial. In contrast, in unINF blocks, a single target was correct for 50 consecutive correct trials (in this example, 'up', indicated by the solid blue arrow). Therefore, whereas in an INF block the monkeys started the trial with decision uncertainty and resolved this uncertainty by viewing the motion, in unINF blocks, the uncertainty was resolved from the outset of the block and the motion provided redundant information. **b**, Example block sequence in a recording session. INF and unINF conditions differed in the probability that one of the targets was correct. In this example, the two targets were 'up' and 'down'. P(up target) is the probability that the up target was correct, and P(down target) = 1 − P(up target). INF and unINF blocks were presented in alternating blocks of 50 correct trials until at least 4 blocks were completed. Small and large RSs were pseudorandomly interleaved within each block. The block type that was presented first (INF or unINF) and the target direction in the first unINF block were randomized across sessions. **c**, The 2 × 2 factorial design dissociating IG and RS. The colors indicate the convention we use throughout the paper, whereby INF blocks are shown in red and unINF blocks in blue, and saturated and pale colors indicate large and small RSs, respectively.

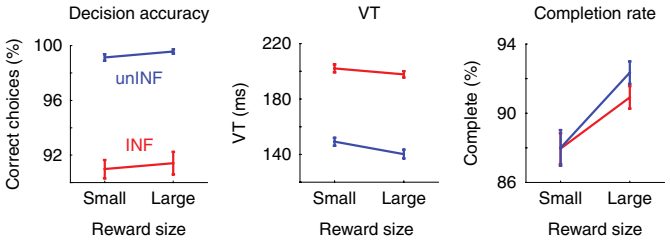

Fig. 2 | Behavior is sensitive to IG. Each point shows the mean and s.e.m. across all neural recording sessions ($n = 87$) with respect to the decision accuracy (the probability of selecting the correct final target), the VT (the time that the monkeys spent viewing the motion before their second saccade) and the completion rate (the fraction of trials in which the monkeys traversed all task states up to the second saccade).

had reward value independently of IG. We further manipulated the reward size (RS) for the second saccade, with large and small rewards randomly interleaved in each block and signaled by the fixation point color (Fig. 1a). This created a 2 × 2 factorial design that statistically dissociated RS and IG (Fig. 1c).

Behavior. The monkeys had higher rates of trial completion at large relative to small RSs (Fig. 2, right; two-way ANOVA, main effect of RS: $F_{(1,344)} = 20.0$, $P < 10^{-5}$), showing that RS impacted their motivation. However, the RS had only a modest influence on the initial cue-directed saccade (Supplementary Fig. 1a) and, importantly, on the monkeys' final decision, including the accuracy (Fig. 2, left; two-way ANOVA, main effect of RS on accuracy: $F_{(1,344)} = 0.6$, $P = 0.4$; IG–RS interaction: $F_{(1,344)} = 10^{-5}$, $P = 1.0$) and the time to make the decision (post-saccadic motion viewing time (VT); Fig. 2, center; two-way ANOVA, main effect of RS on VT: $F_{(1,344)} = 5.5$, $P = 0.02$; IG–RS interaction: $F_{(1,344)} = 0.69$, $P = 0.4$; but see subsequent discussion and Supplementary Fig. 5 for individual monkey behaviors).

In contrast to the weak effects of RS, IG strongly modulated the timing and accuracy of the final decision. In unINF blocks, the monkeys spent minimal time viewing the motion and nevertheless reached very high decision accuracy (Fig. 2, center and left). In contrast, in INF blocks, VTs were significantly longer and decision accuracy levels dropped, showing that the monkeys required more time to link the motion information with the correct final action (Fig. 2; two-way ANOVA, main effect of IG on VT: $F_{(1,344)} = 388$, $P < 10^{-57}$; accuracy $F_{(1,344)} = 222$, $P < 10^{-38}$; all $P < 10^{-24}$ in individual monkeys). Completion rates were insensitive to IG (main effect of IG: $F_{(1,344)} = 0.8$, $P = 0.4$; IG–RS interaction: $F_{(1,344)} = 0.7$, $P = 0.4$), showing that the monkeys were equally motivated to complete the INF and unINF blocks. In contrast with its effects on the final decision, IG had minimal influence on the initial cue-directed saccade (Supplementary Fig. 1a), and there was no negative correlation between the first saccade latency and the post-saccadic viewing durations, ruling out that the monkeys traded off the time they spent preparing the first and second saccades (Supplementary Fig. 1b).

LIP neurons respond more in informative and low-reward trials. To understand the neural mechanisms related to informational actions, we placed the cue in the RF of an LIP cell and focused on its responses during the delay period preceding the initial cue-directed saccade (Fig. 1a, delay/first saccade; see Supplementary Fig. 2 for control geometries). The neurons had visual responses to the onset of the cue, followed by sustained delay period activity until saccade onset (Fig. 3). For many neurons, this pre-saccadic activity differed as a function of IG and RS. Some neurons, like the example cell shown in Fig. 3a, left, responded more strongly in INF blocks relative to unINF blocks but were insensitive to RS. Other cells, like the example shown in Fig. 3a, right, were sensitive to RS. Strikingly, the

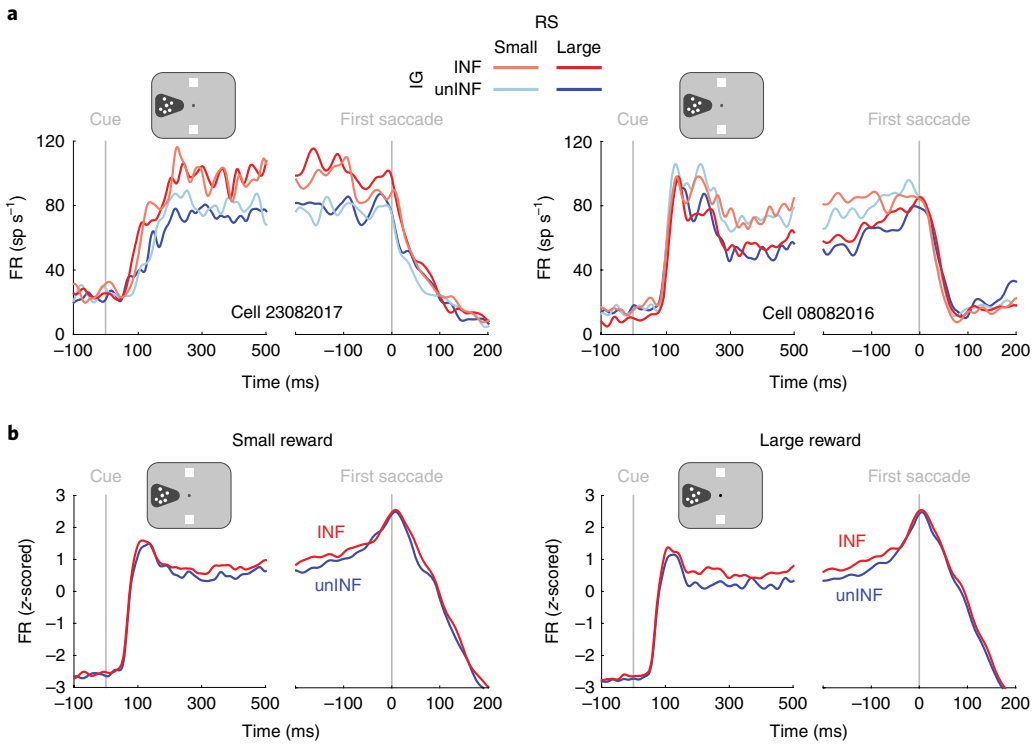

Fig. 3 | Neural responses are stronger in INF blocks and small-reward trials. a, Left: example neuron with stronger responses in the INF blocks relative to the unINF blocks. Peristimulus time histograms (PSTHs) were constructed by convolving trial-by-trial spike trains with a Gaussian filter of 10 ms standard deviation and then averaging across trials. From the time of cue onset (left) throughout the end of the delay period, the monkeys maintained central fixation, and the stationary dots were located inside the RF of the cell (dark cone in the cartoon). At the time of saccade onset (right alignment), the monkeys initiated their first saccade to the dots and the neuron's RF moved away from the visual display. This neuron had higher activity for the INF blocks versus the unINF blocks, with no sensitivity to RS. Right: example neuron with stronger responses for smaller rewards. A different neuron that had higher activity on small reward versus large reward trials but was insensitive to IG. **b**, Population response ($n = 87$ cells). Population PSTHs were constructed by z-scoring the raw FRs within each neuron (using its activity across the entire displayed epoch) and averaging across neurons. For clarity, large and small RSs are shown in separate panels. The population response is larger in the INF context (red versus blue) as for trials with smaller rewards (left versus right).

RS-sensitive cells were typically enhanced by smaller rewards, an effect that was opposite to the enhancement by larger rewards that is commonly observed in this area (for examples, see refs. [10–12]). The average population response ($n = 87$; $n = 49$ in monkey M) showed both effects, with stronger firing rates (FRs) in INF blocks relative to unINF blocks (Fig. 3b, red versus blue) and on small-reward trials relative to large-reward trials (Fig. 3b, left versus right).

To quantitatively measure these modulations, we fitted the delay activity of each cell to a linear model that included IG and RS as categorical regressors, along with nuisance trial-by-trial regressors indicating the first saccade latency, velocity, endpoint accuracy, post-saccadic VT and the direction of the final saccade (Methods, equation (1)). While the sensitivity to saccade parameters was slight (Supplementary Fig. 3a), sizeable fractions of cells showed significant IG and RS modulations. A total of 38% of the cells showed significant effects of RS (Fig. 4; 29% in monkey M, 50% in monkey S). The average β_{RS} coefficient was negative across the population (Fig. 4, upper black triangle; mean (s.e.m.) −1.7 (0.35) spikes per second (sp s^{-1}), $z = -4.6$, $P < 10^{-5}$ relative to 0; monkey M: $z = -3.1$, $P = 0.0022$; monkey S: $z = -3.3$, $P = 0.0011$) and in 79% of the RS-sensitive cells (teal triangle: −3.3 (0.8) sp s^{-1}, $z = -3.4$, $P < 10^{-4}$; 85% in monkey M, 74% in monkey S), indicating that the predominant response was enhancement for a smaller RS. Significant effects of IG were found in 39% of the cells (Fig. 4, ordinate; 47% in monkey M, 29% in monkey S). The IG coefficient was positive across the population (Fig. 4, right black triangle; 2.3 (0.6) sp s^{-1}, $z = 4.2$, $P < 10^{-4}$ relative to 0; monkey M, $z = 3.7$, $P = 0.0002$; monkey S: $z = 2.0$, $P = 0.05$), and in 85% of the significant cells (orange triangle: 5.5 (1.2) sp s^{-1}, $z = 3.8$, $P < 10^{-4}$; 91% in monkey M, 73% in monkey S), which indicates that most cells had higher FRs for INF blocks relative to unINF blocks.

We conducted several analyses to estimate the reliability of these neural effects. In the significant cells, the average RS and IG coefficients represented a change of more than 10% relative to the average FR of the neurons (mean (s.e.m.) for RS: −11% (2.7%), IG: 13% (2.4%)) and more than 35% of the FR standard deviation (RS: −0.36 (0.08) z-score units; IG: 0.43 (0.08) z-score units). The results were replicated when using receiver operating characteristic analysis, which revealed significant discrimination across the population (Supplementary Fig. 3b; RS: mean (s.e.m.) 0.55 (0.011), $z = 4.0$, $P < 10^{-4}$, IG: 0.55 (0.012), $z = 4.0$, $P < 10^{-4}$) and in a sizeable fraction of cells (RS: 38%; IG: 44%). Time-resolved analysis showed that the sensitivity to IG was significant throughout the delay period (Supplementary Fig. 3c). Finally, the variance in FRs was smaller in unINF blocks relative to INF blocks, which is consistent with the lower FRs in the latter blocks, but at odds with the idea that these blocks reflected mixtures of states related to the two anticipated directions of the final saccade (Supplementary Fig. 3d,e).

IG responses are not value effects. We conducted several analyses to determine whether the IG modulations were explained by the reward sensitivity shown by the cells. In a first analysis, we tested whether the cells encode the expected value (EV) of the initial saccade, which is defined as the product of RS and reward rate in each type of block (Fig. 5a). The EV primarily depended on RS, as intended in the design of the task, and was larger in unINF blocks relative to

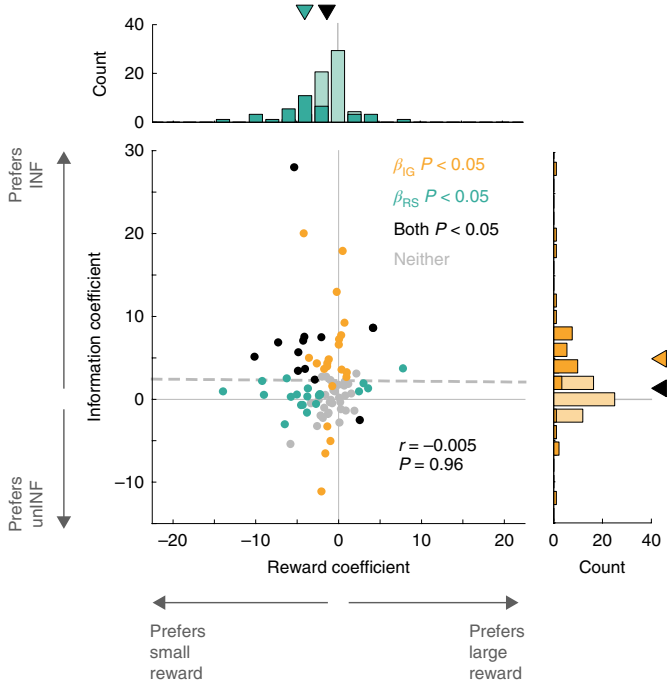

Fig. 4 | Distribution of IG and RS effects in individual cells. Coefficients of a regression model (Methods, equation (1)) capturing the effects of IG in units of sp s^{-1} (β_{IG}; ordinate) and RS (β_{RS}; abscissa). Each point represents one cell ($n = 87$), and colors indicate the significance of the two coefficients. In the marginal distributions, significant cells are indicated in darker shades and the arrowheads indicate the average values across the entire sample (black) and the subset of cells with significant coefficients (teal or orange). The gray vertical and horizontal lines show the null effects ($\beta_{IG} = 0$ and $\beta_{RS} = 0$). The broken line represents the least square regression, and the *r* and *P* values refer to the correlation coefficient relating the IG and RS coefficients.

INF blocks because of the higher decision accuracy in the former blocks (Fig. 5a). Thus, the EV showed significant positive effects of RS and IG, and a negative IG–RS interaction (two-way ANOVA, RS main effect: $F_{(1,344)} > 1{,}060$, $P < 10^{-50}$ for the full dataset and each monkey; IG main effect: all $F_{(1,344)} > 90$, $P < 10^{-18}$; IG–RS interaction: all $F_{(1,344)} > 8.5$, $P < 10^{-3}$). This pattern was qualitatively different from the average LIP FRs, which showed a negative effect of RS and no IG–RS interaction (Fig. 5c; two-way ANOVA, main effects of IG and RS: both $F_{(1,344)} > 39$, $P = 10^{-9}$; $F_{(1,344)} > 7$, $P < 0.01$ in each monkey individually; interaction: $F_{(1,344)} = 1.3$, $P = 0.3$; monkey M: $F_{(1,344)} = 1.8$, $P = 0.2$; monkey S: $F_{(1,344)} = 0.03$, $P = 0.9$).

We next examined whether the cells encode the value of information (VOI)—a higher order reward function that measures the added value of obtaining information relative to what the monkeys may expect to obtain had they acted without the information. The monkeys could have estimated the VOI based on their experience with catch trials, in which no motion was shown and the monkeys acted based on their prior expectations (10% in each block; Methods). Catch trials had high success rates of 93% in unINF blocks (96% in monkey M, 90% in monkey S), but were only at chance rates in INF blocks (49% overall; 53% in monkey M, 49% in monkey S), consistent with the different levels of ex ante uncertainty in the two types of blocks. Thus, VOI—the difference in EV between motion and no-motion (catch) trials—was very low in unINF blocks regardless of RS, but it was positive in INF blocks, particularly at higher RS (Fig. 5b; two-way ANOVA, $F_{(1,344)} > 470$, $P < 10^{-47}$ for main effect of IG, RS and IG–RS interactions, in the full dataset and each monkey). The strong positive interaction between IG and RS distinguishes VOI from EV (which shows a negative interaction; Fig. 5a) and from uncertainty reduction per se (which is independent of reward magnitude). Importantly, this pattern also distinguishes VOI from the LIP pre-saccadic response, in which IG and RS were encoded additively and with opposite signs (Fig. 5a).

These findings were confirmed by examination of individual cells. We reasoned that, if the IG effects were fully explained by reward sensitivity, the two signals would be highly correlated, such that neurons would only show IG sensitivity if they also had reward modulations. Contrary to this view, β_{IG} and β_{RS} coefficients were uncorrelated (Fig. 4; $r = -0.0051$, $P = 0.96$; monkey M: $r = -0.009$, $P = 0.95$; monkey S: $r = -0.11$, $P = 0.5$). To rule out that this negative result was an artifact of low statistical power, we estimated the β_{IG} separately for small-reward trials and large-reward trials—that is, using only half the number of trials for each cell. The resulting β_{IG} coefficients were highly correlated across small-reward trials and large-reward trials ($r = 0.76$, $P < 10^{-17}$; monkey M: $r = 0.79$, $P < 10^{-10}$; monkey S: $r = 0.51$, p 0.0011). This result shows that we could detect reliable correlations even if we used half the number of trials, and confirms that the lack of correlation between the IG and RS modulations reflects a true independence of the two modulations.

Because both EV and VOI measures showed prominent interactions between RS and IG, we repeated the individual neuron analysis using a model that included IG, RS and the IG–RS interaction (Methods, equation (2)). In contrast to the EV and VOI, the interaction coefficients in LIP FRs did not differ from 0 across the population (Fig. 5d; β_{INT} mean (s.e.m.) = 0.44 (0.42), $z = 1.6$, $P = 0.11$; monkey M: 0.34 (0.63), $z = 1.4$, $P = 0.15$; monkey S: 0.58 (0.51), $z = 0.6$, $P = 0.56$) and the β_{IG} coefficients were equivalent whether the regression model did or did not include an interaction term (Fig. 5e; $z = 1.42$, $P = 0.16$; $r = 0.94$, $P < 10^{-40}$).

We further evaluated these observations at the population level by fitting the population responses with the full set of 127 models that resulted from all the possible combinations of 7 regressors, including categorical indicators of task context (IG, RS and IG–RS) and average EV, VOI, decision accuracy and completion rates in individual sessions (Fig. 2). The best-fitting model was a two-parameter model that included only terms for IG and RS (Supplementary Fig. 4). Consistent with the individual-neuron results, this model produced a significantly positive effect of IG and a negative effect of RS ($\beta_{IG\_population}$ (s.e.m.): combined data: 0.17 (0.016); monkey M: 0.24 (0.022); monkey S: 0.079 (0.024), all $P < 0.05$; $\beta_{RS\_population} = -0.17$ (0.016); monkey M: −0.094 (0.02); monkey S: −0.26 (0.024); all $P < 0.05$). A three-parameter model with IG, RS and IG–RS as regressors produced an inferior fit and a nonsignificant interaction coefficient ($P = 0.09$). Finally, the models with the lowest Bayesian information criterion scores included the IG and RS terms, but only inconsistently included other predictors (Supplementary Fig. 4, bold). In summary, at the level of the population and individual cells, LIP FRs are best described as encoding IG and RS, rather than reward gains or behavioral indicators that covaried with context.

LIP responses to IGs correlate with post-saccadic discrimination efficacy. Since the neurons showed enhanced pre-saccadic FRs when the task required more engagement during the post-saccadic fixation, we tested whether the IG modulations were related to the efficacy of the post-saccadic motion discrimination. To this end, we plotted the accuracy of the final decision as a function of post-saccadic VT (Fig. 6a,b). Decision accuracy in unINF blocks was near the ceiling regardless of VT (Supplementary Fig. 5, blue). However, accuracy and VT in INF blocks were positively related (Fig. 6a,b), showing that, although the motion was fully coherent, the monkeys needed time to select the appropriate action. A median split of the data based on the neural β_{IG} coefficient showed that the increase in accuracy was steeper in sessions in which the recorded neurons had stronger IG modulations (Fig. 6a, black versus gray). Note that this

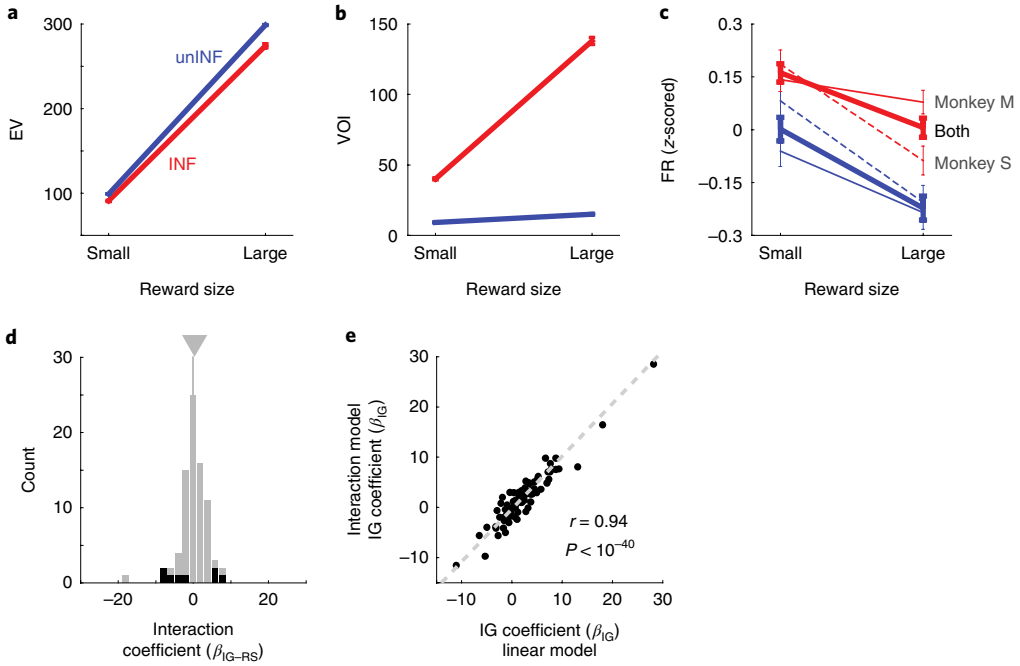

Fig. 5 | IG signals cannot be explained by the VOI or the EV. a, The EV experienced by the monkeys. We estimated the EV as the product of RS and decision accuracy. **b**, The VOI experienced by the monkeys, measured as the difference in EV between trials in which the monkeys viewed the dot motion and catch trials, in which the motion was absent and the monkeys guessed the direction of the final saccade. Each point shows the average and s.e.m. across sessions ($n=87$). **c**, Population-level FRs were inconsistent with the VOI or the EV. Each point is the mean and s.e.m. FR during the delay period in the full dataset (thick traces; n = 87 cells) and individual monkeys (thin traces). **d**, The majority of neurons do not show IG–RS interactions. The distribution of interaction coefficients from the three-parameter model. Significant coefficients were found in only eight cells (black bars), of which only three were positive. The gray triangle shows the mean coefficient and the vertical line shows the abscissa = 0. **e**, INF coefficients are equivalent when estimated with the two-parameter and three-parameter models. Each point represents one cell ($n=87$). The broken diagonal line is the best fit least squares linear regression.

effect involves a comparison across distinct groups of cells, which suggests that the relationship between β_{IG} and performance is a network effect—that is, it can be detected above and beyond the specific sample of neurons that we happened to record in a session.

Interestingly, the relationship between decision efficiency and the β_{IG} coefficient was prominent in large-reward trials but not small-reward trials (Fig. 6a, inset). A two-way analysis of covariance with VT as a continuous covariate confirmed that the β_{IG} had a significant effect on accuracy above and beyond the effect of VT (Lawley–Hotelling trace $T=12.71$, $P=0.0055$), and the relationship was stronger on large-reward trials relative to small-reward trials (RS–β_{IG} interaction: $T=7.0$, $P=0.0084$), even though the VT showed no effect of RS (main effect of RS: $T=2.8$, $P>0.4$; RS–VT interaction: $T=0.6$, $P>0.3$ in the combined data and individual monkeys). In contrast to the effects of IG, performance did not differ when the data were split according to β_{RS} irrespective of whether we examined low-reward trials, high-reward trials or both (Fig. 6b; effects of β_{RS}, VT–β_{RS} and RS–β_{RS} all $T<2.0$, $P>0.1$ overall and in individual monkeys). Therefore, the efficiency of the post-saccadic discrimination is not related to the LIP reward modulations but is related to the neuronal IG sensitivity in a reward-dependent fashion.

Our earlier finding that the neurons did not encode variations in post-saccadic VT (Supplementary Fig. 2) suggests that, while LIP firing correlates with decision efficiency at a constant VT, it may not encode speed–accuracy trade-offs across the different contexts. To directly examine this hypothesis, we examined how the monkeys traded off VT and accuracy for different RSs in INF blocks. The two monkeys made different adjustments in response to RS. Monkey M slowed down and became more accurate on large-reward trials relative to small-reward trials, whereas monkey S showed the opposite pattern, making faster and less accurate responses when higher rewards were at stake (Supplementary Fig. 5). We captured this difference by calculating a combined index of speed and accuracy and taking the difference between the indices on large-reward trials versus small-reward trials (Fig. 6c; Supplementary Fig. 5). Monkey M showed a positive difference on average, which indicates that he slowed down and achieved higher accuracy on large-reward trials versus small-reward trials (Fig. 6c, abscissa, median difference (s.e.m.) = 3.1 (1.48), $z=2.5$, $P=0.013$ relative to 0). Monkey S showed a negative difference, which indicates that he sped up and sacrificed accuracy when larger rewards were at stake (a.u., median difference (s.e.m.) = −11.3 (3.04), $z=3.5$, $P=0.00049$ relative to 0). This behavioral difference was highly significant ($z=4.1$, $P<10^{-5}$ between the two monkeys), but was uncorrelated with the LIP response. The behavioral index was not correlated with the magnitude of the RS sensitivity ($r=0.0072$, $P=0.51$ overall; monkey M: $r=-0.077$, $P=0.6$; monkey S: $r=0.012$, $P=0.94$) or with the difference between the IG coefficient for small and large RSs (Fig. 6c; $r=0.089$, $P=0.41$ overall; monkey M: $r=0.059$, $P=0.69$; monkey S: $r=0.13$, $P=0.44$). Therefore, LIP responses are correlated with behavior in a very specific fashion via an increase in decision efficiency as a function of the strength of the IG effect independently of speed–accuracy strategies.

Negative reward effects are explained by the task. Our finding that the neurons had negative reward modulations was unexpected given that previous studies have reported that the cells have higher FRs for higher rewards. This raised the possibility that we may have inadvertently recorded from a different population of cells. Two

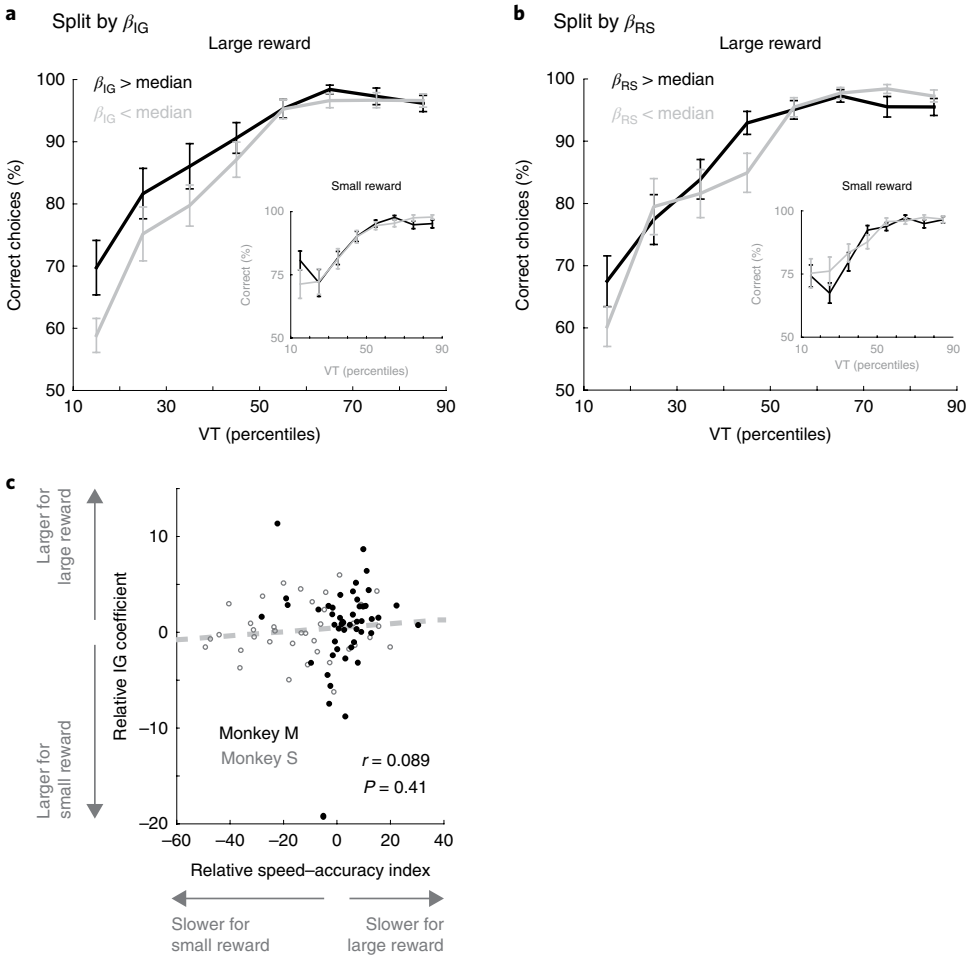

Fig. 6 | The strength of IG signals correlates with performance. a, For a fixed VT, stronger IG modulations are associated with higher decision accuracy. The distribution of INF trials for each RS was divided into deciles according to the VT, and mean decision accuracy was plotted as a function of deciles ($n = 87$, error bars show s.e.m.), separately for neurons showing large or small β_{IG} (median split). Decision accuracy was higher in sessions in which neurons had higher β_{IG} values. This difference was found on large-reward trials (main panel) but not small-reward trials (inset). **b**, Stronger RS modulations are not related to higher decision accuracy. Same format as in **a**, but splitting sessions according to the β_{RS} of the recorded cell. Note that β_{RS} > median means a weaker reward effect (less-negative coefficient). **c**, IG modulations do not correlate with speed accuracy trade-offs. Each point represents one session ($n = 87$), with the color denoting individual monkeys. The abscissa shows the difference between the speed–accuracy index (calculated as described in Supplementary Fig. 5) on large-reward trials relative to small-reward trials. The ordinate is the difference between the β_{IG} on the same trials. The broken diagonal line is the least square regression; the *r* and *P* values refer to the correlation coefficients.

observations strongly argue against this possibility. First, all the neurons that were tested with the two-step task were pre-screened using a memory-guided saccade (MGS) task and showed spatially tuned delay period activity, thus conforming to the functional definition of LIP cells[13,14] (Supplementary Fig. 6; population: $z = 8.0$, $P < 10^{-14}$ overall; $z > 5.1$, $P < 10^{-7}$ in individual monkeys; $P < 0.05$ in 93% of individual cells).

For additional confirmation, we tested a subset of the cells on a traditional one-step saccade task in which the monkeys made a single saccade to receive a large or small reward (with RSs equated to those in the two-step task; see Methods for details). Replicating the findings in the entire sample, the cells tested in this control task ($n = 56$ out of 87) showed a significant enhancement by small RSs during the delay period of the two-step task (β_{RS} average (s.e.m.) = −1.8 (0.5) sp s^{-1}, $z = -3.1$, $P = 0.002$, $n = 56$). When tested with the one-step task, however, the same neurons had a positive reward effect, as previously shown for this area (Fig. 7a; a 200-ms window centered on saccade onset; mean $\beta_{RS\_one\text{-}step} = 2.7$ (1.2), $z = 2.2$, $P = 0.025$ relative to 0; $z = 3.7$, $P = 0.0002$ relative to the delay period of the two-step task).

We finally tested whether the neurons showed reward enhancement for the final saccade in the two-step task. However, even though this saccade collected the final reward, the 48 cells that were tested in control geometry 2 (Supplementary Fig. 2c) showed no effect of RS in this epoch (Fig. 7b; mean (s.e.m.) = −0.46 (0.73), $z = -1.21$, $P = 0.22$, $n = 48$) and no correlation between the RS coefficients before the first and second saccades of the two-step task ($r = -0.01$, $P = 0.92$, overall; monkey M: $r = 0.09$, $P = 0.64$; monkey S: $r = -0.19$, $P = 0.46$). Similar to the entire sample, these cells showed a significant enhancement with the larger rewards in the one-step task (mean (s.e.m.) = 3.0 (1.3), $z = 2.04$, $P = 0.04$) and a significant difference between the one-step and two-step tasks ($z = 2.25$, $P = 0.02$). Thus, the discrepancy between our results and previous investigations is explained by the behavioral context and not the neuronal population we sampled.

IC effects do not encode uncertainty, arousal or difficulty. To determine whether the IG modulations reflect nonspecific differences between the INF and unINF contexts, we compared the modulations related to the cue/initial saccade with those related to

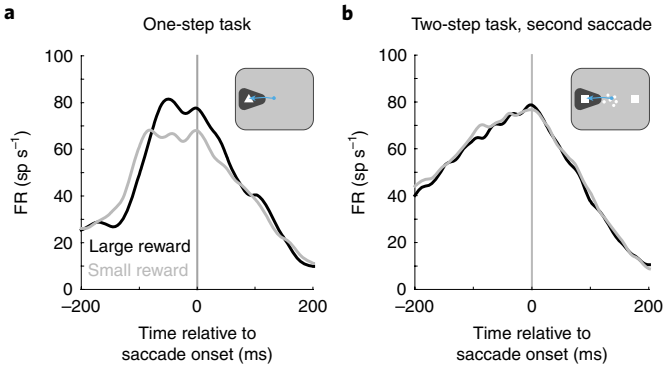

Fig. 7 | LIP neurons are enhanced by reward in a traditional one-step task. **a**, Saccade-aligned population PSTHs on the standard one-step task. The cartoon shows the task geometry, which involved a single saccade to a target inside the RF, with the expectation of a large or small reward. **b**, Saccade-aligned population PSTHs in the same format as in **a**, but for the second saccade of the two-step task (control geometry 2; Supplementary Fig. 2c).

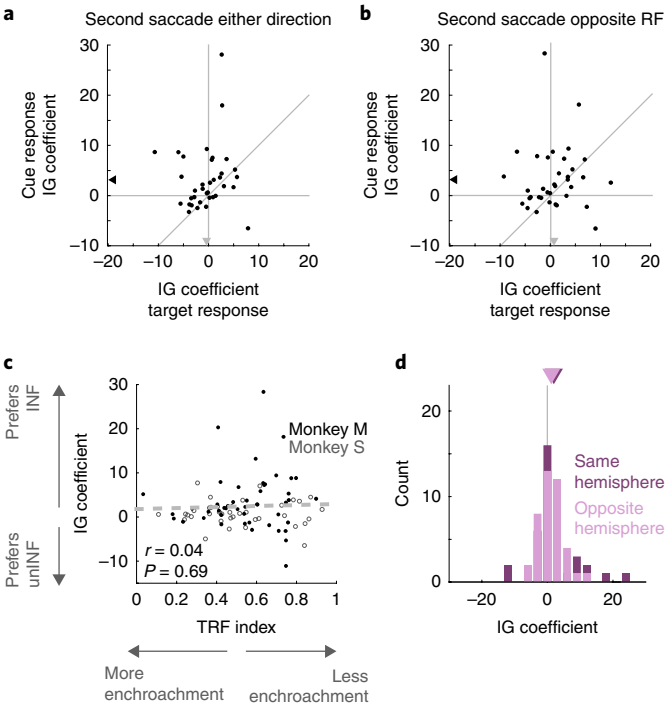

Fig. 8 | Controls ruling out alternative explanations. **a**, IG modulations are specific rather than global effects. Comparison of IG coefficients in response to the cue (standard geometry) and to the targets during the delay period (geometry 1; Supplementary Fig. 2b). Each point represents one cell ($n=36$). The diagonal line is the equality line. Arrowheads show the marginal means, black if $P<0.05$, otherwise gray. During the delay period, the IG modulates responses to the cue/first saccade (black) but not the responses to the target in geometry 1 (gray). **b**, IG effects are not by-products of spatial competition. Comparison of β_{IG} in response to the cue (standard geometry) and to the target when it is opposite the RF in unINF blocks (geometry 1; Supplementary Fig. 2b). Each point represents one cell ($n=36$). The diagonal line is the equality line. Arrowheads show marginal means, black if $P<0.05$, otherwise gray. Contrary to the spatial competition hypothesis, the neurons did not show IG modulations when the final saccade target was out of the RF. **c**, IG modulations do not depend on the relative distance between the cue and targets. The IG coefficient (β_{IG}, ordinate) as a function the TRF index measuring the relative responses to the locations occupied by the cue and the target in the standard geometry (Methods, equation (3)). Larger values along the abscissa indicate cells for which the target elicited a stronger response; larger values along the ordinate indicate cells with stronger IG sensitivity. Each point represents one cell ($n=87$), and color denotes individual monkeys. The broken diagonal line is the least square regression; the r and P values refer to the correlation coefficients. **d**, IG modulations do not depend on the visual hemifield locations of the cue and targets. Comparison of the β_{IG} coefficients in trials in which the final saccade was directed to the same versus the opposite hemifield relative to the cue, for cells that had a target in each hemifield ($n=41$). Arrowheads show marginal means.

the targets of the final saccade. We reasoned that if the IG modulations were nonspecific effects of uncertainty, arousal or difficulty, they should be found not only for the cue but also the target-related responses[15]. We therefore used control geometry 1, which revealed how the neurons encoded the saccade targets during the delay period preceding the initial saccade (Supplementary Fig. 2b) and computed the IG modulations in this geometry, pooling across saccade directions to detect nonspatial effects (Fig. 8a). The neurons did not show significant IG modulations in their target-related response (Fig. 8a abscissa; β_{IG_target} mean (s.e.m.) = −0.31 (0.64), $z=0.41$, $P=0.68$ relative to 0; $n=36$) and had much larger IG coefficients in the cue-related response relative to the target-related response ($z=3.21$, $P=0.0014$; cue-related IG: β_{IG_cue} mean (s.e.m.) = 3.2 (1.1), $z=2.9$, $P=0.0038$ relative to 0; $n=36$). Thus, the IG modulations were specific to the visual cue rather than indicating global changes of gain in the INF context.

IG effects cannot be explained by spatial normalization. A final hypothesis we considered is that the IG modulations arose indirectly from spatial competition between pools of LIP neurons that encode plans for the first and second saccade. According to this view, IG modulations may arise because the monkeys could plan their second saccade as early as the delay period in the unINF but not in the INF blocks. If the neurons encoded this advance saccade plan, this might have triggered competitive interactions that reduced the responses to the first saccade specifically in the unINF blocks, thus masquerading as an IG effect. Several analyses argue against this interpretation.

We reasoned that an IG effect produced by spatial competition would also be seen in the neural responses to the targets. Crucially, neurons should show an apparent IG effect in trials in which the final saccade was away from the RF, as the advance planning of the null-direction saccade would produce lower activity in the unINF blocks relative to the INF blocks. We therefore evaluated the IG coefficient in control geometry 1 as we did for the data shown in Fig. 8a, but this time separately for unINF blocks with different saccade directions (Fig. 8b). Contrary to the spatial competition hypothesis, the neurons did not show IG modulations when the final saccade target was out of the RF (Fig. 8b, abscissa; mean 0.66 (0.76), $z=0.72$, $P=0.47$ relative to 0), and the IG coefficients in this condition were uncorrelated with and significantly lower than the cue-related effects ($r=0.04$, $P=0.81$; $z=2.2$, $P=0.028$ paired comparison; cue-related coefficient in this subset of cells was 3.2 (1.1), $z=2.9$, $P=0.0038$ relative to 0, $n=36$). Similar results were obtained when using unINF blocks in which the final saccade was toward the RF (mean IG coefficient = −1.7 (0.95), $z=-1.9$, $P=0.06$ relative to 0; relative to cue-related IG: $z=3.4$, $P<10^{-3}$ paired comparison; $r=0.16$, $P=0.35$).

A second important prediction stems from the fact that competitive interactions between stimuli depend strongly on the overlap in their neural representations, implying that the IG modulations should be inversely related to the distance between the cue and the targets[16,17]. The relevant distance may be defined by the neural

representation—that is, the extent to which the cue and target locations activate the same population of cells. To test this hypothesis, we used RF mapping data from the MGS task to compute a target RF (TRF) index that ranged between 1 (indicating a cell for which the target location was entirely outside the RF) and 0 (indicating a cell for which the target location strongly encroached on the RF, eliciting responses equivalent to cue location; Methods, equation (3)). If the IG sensitivity arose from spatial competition, it should be inversely correlated with the TRF—that is, be larger for neurons whose RFs included both the cue and target locations. However, no such correlation was present in the neural response (Fig. 8c; $r=0.044$, $P=0.69$ overall; monkey M: $r=0.083$, $P=0.57$; monkey S: $r=-0.12$, $P=0.46$).

An alternative version of this hypothesis is that the relevant distance is relative to the visual field and that competition is strongest when the cue and target locations fall within the same, relative to opposite, hemifields. To evaluate this possibility, we focused on neurons for which the cue was at a diagonal location (did not fall on the vertical or horizontal meridians) and the two saccade targets fell in opposite hemifields. If the IG sensitivity were due to visual competition, it should be stronger when the monkeys planned the second saccade to the target that occupied the same hemifield rather than the opposite hemifield relative to the cue. Contrary to this prediction, the β_{IG} values were highly correlated and statistically equivalent between the two geometries (Fig. 8d; $z=0.21$, $P=0.83$ between the two conditions ($n=41$); monkey S: $z=0.12$, $P=0.91$; monkey M: $z=0.4$, $P=0.69$). In summary, neither the temporal nor the spatial properties of the IG modulations are consistent with a spatial interaction hypothesis.

Discussion

In contrast to laboratory tasks in which participants make saccades to gather rewards, in this experiment we focused on the neural correlates of saccades that gathered information. In a previous study[8] using this paradigm, we showed that LIP neurons encoded expected IGs based on fixed, long-term estimates of cue validity. Here, we extend this result by showing that the cells are also sensitive to expected IGs occasioned by dynamic changes in decision uncertainty. Responses to decision uncertainty are found in frontal cortical areas[18,19] and subcortical structures, including dopamine cells[20–22], and have been implicated in reward expectation, confidence and risk attitudes (for example, see ref. [23]). Our findings suggest that these responses also play key roles in determining the informativeness of sensory cues, thus raising important new questions about the neural links between decision uncertainty, attention and active sensing strategies[2,24–26].

Given the dual sensitivity of LIP cells to rewards and saccadic decisions, it seems natural to propose that the cells encode the economic utility of competing alternatives[10,11]. Our results argue against this interpretation and argue instead that the apparent encoding of economic utility may be limited to laboratory tasks in which animals make saccades directly to collect a reward. Although LIP cells had the expected reward-related enhancement in a traditional one-step saccade task, they showed no reward sensitivity for the final saccade of the two-step task and, strikingly, showed enhancement for smaller rewards before the information-sampling saccade in this task. Moreover, the neural sensitivity to IGs could not be explained by the reward value of gathering information. In striking contrast to the value hypothesis—which predicts that the neural sensitivity to IGs and reward gains should be correlated, interact multiplicatively rather than additively, and have congruent signs—the sensitivities of the neurons to reward and IG were uncorrelated, combined additively and, critically, had opposite signs (increasing as a function of IG but decreasing with reward gains).

In contrast to their inconsistent encoding of utility, the neural sensitivity to IGs correlated with the efficiency with which the monkeys used the information in the post-saccadic fixation—as measured by the decision accuracy at a given VT. This relationship differed from attentional interpretations of LIP function in two significant ways. First, contrary to the traditional view that top-down attentional feedback facilitates visual discrimination in a retinotopic fashion within a single fixation[5,16], the facilitatory effect in our task was non-retinotopic and linked the neural responses to a peripheral location before the saccade with motion processing at a foveal location after the saccade. Second, in contrast with the prevailing pre-motor view of attention, whereby attention is recruited merely in relation to a saccade motor plan[5], the effects we describe here link the LIP pre-saccadic responses with the cognitive demands of the post-saccadic fixation.

These findings suggest that current views based on economic utility or attentional priority are insufficient to describe the neural mechanisms of information-sampling decisions. Instead, we propose that understanding this process requires a broader framework that integrates oculomotor decisions and cognitive control mechanisms. Specifically, our results support the expected value of control (EVC) theory that postulates a separation between monitoring and regulative (implementation) aspects of control[9].

According to the EVC theory, the dorsal anterior cingulate cortex (dACC) monitors the rewards and costs of alternative actions and uses this information to decide whether to engage in a task and how much effort (control) to allocate to the task. The control signal generated by the dACC then recruits more posterior 'regulatory' areas, including lateral frontal and parietal areas[27,28], to implement the required level of effort. The dACC is proposed to call for additional effort by boosting neuromodulators—including dopamine and norepinephrine[29]—which may have led to the enhanced neural gain we observed in conditions of higher uncertainty. In this view, 'attentional priority' is a type of focused arousal; that is, a transformation of global arousal into a stimulus-specific gain increase, which enables animals to efficiently reduce uncertainty by focusing on and extracting the information delivered by relevant cues.

This idea naturally accounts for the fact that the effects of IG in our task were mere modulatory effects on the larger visual and pre-saccadic responses of the neurons. The effects we describe are comparable to previously reported attentional and reward modulations[14,30,31] and, although they seem modest in size, the fact that they correlate with behavioral efficiency suggests that they are functionally significant. If our hypothesis is correct, it implies that a full understanding of the functional consequences of IG-related enhancements requires an understanding of the large-scale networks that control active sampling; these networks include the dACC and possibly also the orbitofrontal cortex and dopamine cells that seem to signal information value in tasks motivated by curiosity[32,33], along with downstream readout mechanisms that translate these responses into actions[34].

The interpretation of priority maps as implementing cognitive effort may also explain our present result that the cells scaled negatively with reward magnitude. In experiments that randomly interleave small and large RSs, a smaller reward is perceived as a loss and elicits prepotent 'escape' reactions in both behavior and neural responses known as motivational conflict[35,36]. Motivational conflict was also seen in the behavior of our monkeys, as the rates of trial completion were smaller for lower rewards (Fig. 2). If resolving the conflict and completing a low-reward trial requires enhanced cognitive effort, this may explain the stronger responses for smaller RSs that we observed. The need for enhanced control in conditions of conflict can parsimoniously explain other seemingly paradoxical findings in LIP cells, including the fact that the cells have enhanced responses to punishment-predicting cues that monkeys must look away from[37] or to stimuli signaling visuomotor conflict such as an antisaccade[38] or a change in motor effector[39]. Should this hypothesis be correct, our finding that responses to RS and IG are uncorrelated

suggests that different types of effort (for example, related to uncertainty reduction, visuomotor conflict or motivational conflict) require boosting through distinct circuits, which is consistent with a recent report[40]. Thus a central question for future investigation concerns the relation between priority maps, value and cognitive effort in implementing active sensing strategies.

Online content

Any methods, additional references, Nature Research reporting summaries, source data, statements of code and data availability and associated accession codes are available at https://doi.org/10.1038/s41593-019-0440-1.

Received: 3 October 2018; Accepted: 28 May 2019;
Published online: 8 July 2019

References

1. Hanks, T. D. & Summerfield, C. Perceptual decision making in rodents, monkeys, and humans. *Neuron* **93**, 15–31 (2017).
2. Gottlieb, J. & Oudeyer, P. Y. Toward a neuroscience of active sampling and curiosity. *Nat. Rev. Neurosci.* **19**, 758–770 (2018).
3. Gottlieb, J. Understanding active sampling strategies: empirical approaches and implications for attention and decision reseeaerch. *Cortex* **17**, 30276–30279 (2017).
4. Gottlieb, J., Hayhoe, M., Hikosaka, O. & Rangel, A. Attention, reward and information seeking. *J. Neurosci.* **34**, 15497–154504 (2014).
5. Bisley, J. W. & Goldberg, M. E. Attention, intention, and priority in the parietal lobe. *Annu. Rev. Neurosci.* **33**, 1–21 (2010).
6. Thompson, K. G. & Bichot, N. P. A visual salience map in the primate frontal eye field. *Prog. Brain Res.* **147**, 251–262 (2005).
7. Maunsell, J. H. Neuronal representations of cognitive state: reward or attention? *Trends Cogn. Sci.* **8**, 261–265 (2004).
8. Foley, N. C., Kelley, S. P., Mhatre, H., Lopes, M. & Gottlieb, J. Parietal neurons encode expected gains in instrumental information. *Proc. Natl Acad. Sci. USA* **114**, E3315–E3323 (2017).
9. Shenhav, A., Botvinick, M. & Cohen, J. The expected value of control: an integrative theory of anterior cingulate cortex function. *Neuron* **79**, 217–240 (2013).
10. Kable, J. W. & Glimcher, P. W. The neurobiology of decision: consensus and controversy. *Neuron* **63**, 733–745 (2009).
11. Sugrue, L. P., Corrado, G. S. & Newsome, W. T. Choosing the greater of two goods: neural currencies for valuation and decision making. *Nat. Rev. Neurosci.* **6**, 363–375 (2005).
12. Peck, C. J., Jangraw, D. C., Suzuki, M., Efem, R. & Gottlieb, J. Reward modulates attention independently of action value in posterior parietal cortex. *J. Neurosci.* **29**, 11182–11191 (2009).
13. Barash, S., Bracewell, R. M., Fogassi, L., Gnadt, J. W. & Andersen, R. A. Saccade-related activity in the lateral intraparietal area. I. Temporal properties. *J. Neurophysiol.* **66**, 1095–1108 (1991).
14. Sugrue, L. P., Corrado, G. S. & Newsome, W. T. Matching behavior and the representation of value in the parietal cortex. *Science* **304**, 1782–1787 (2004).
15. Aston-Jones, G. & Cohen, J. D. An integrative theory of locus coeruleus-norepinephrine function: adaptive gain and optimal performance. *Annu. Rev. Neurosci.* **28**, 403–450 (2005).
16. Reynolds, J. H. & Heeger, D. J. The normalization model of attention. *Neuron* **61**, 168–185 (2009).
17. Balan, P. F., Oristaglio, J., Schneider, D. M. & Gottlieb, J. Neuronal correlates of the set-size effect in monkey lateral intraparietal area. *PLoS Biol.* **6**, e158 (2008).
18. O'Neill, M. & Schultz, W. Coding of reward risk by orbitofrontal neurons is mostly distinct from coding of reward value. *Neuron* **68**, 789–800 (2010).
19. Tobler, P. N., Christopoulos, G. I., O'Doherty, J. P., Dolan, R. J. & Schultz, W. Risk-dependent reward value signal in human prefrontal cortex. *Proc. Natl Acad. Sci. USA* **106**, 7185–7190 (2009).
20. Monosov, I. E., Leopold, D. A. & Hikosaka, O. Neurons in the primate medial basal forebrain signal combined information about reward uncertainty, value, and punishment anticipation. *J. Neurosci.* **35**, 7443–7459 (2015).
21. Monosov, I. E. & Hikosaka, O. Selective and graded coding of reward uncertainty by neurons in the primate anterodorsal septal region. *Nat. Neurosci.* **16**, 756–762 (2013).
22. Schultz, W. et al. Explicit neural signals reflecting reward uncertainty. *Philos. Trans. R. Soc. Lond. B Biol. Sci.* **363**, 3801–3811 (2008).
23. Pouget, A., Drugowitsch, J. & A., K. Confidence and certainty: distinct probabilistic quantities for different goals. *Nat. Neurosci.* **19**, 366–374 (2016).
24. Fan, J. An information theory account of cognitive control. *Front. Hum. Neurosci.* **8**, 680 (2014).
25. Vossel, S. et al. Spatial attention, precision, and bayesian inference: a study of saccadic response speed. *Cereb. Cortex* **24**, 1436–1450 (2014).
26. Dayan, P., Kakade, S. & Montague, P. R. Learning and selective attention. *Nat. Neurosci.* **3** (Suppl.), 1218–1223 (2000).
27. Krebs, R. M., Boehler, C. N., Roberts, K. C., Song, A. W. & Woldorff, M. G. The involvement of the dopaminergic midbrain and cortico–striatal–thalamic circuits in the integration of reward prospect and attentional task demands. *Cereb. Cortex* **22**, 607–615 (2012).
28. Chong, T. T. et al. Neurocomputational mechanisms underlying subjective valuation of effort costs. *PLoS Biol.* **15**, e1002598 (2017).
29. Silvetti, M., Vassena, E., Abrahamse, E. & Verguts, T. Dorsal anterior cingulate–brainstem ensemble as a reinforcement meta-learner. *PLoS Comput. Biol.* **14**, e1006370 (2018).
30. Bisley, J. W. & Goldberg, M. E. Neuronal activity in the lateral intraparietal area and spatial attention. *Science* **299**, 81–86 (2003).
31. Louie, K., Grattan, L. E. & Glimcher, P. W. Reward value-based gain control: divisive normalization in parietal cortex. *J. Neurosci.* **31**, 10627–10639 (2011).
32. Blanchard, T. C., Hayden, B. Y. & Bromberg-Martin, E. S. Orbitofrontal cortex uses distinct codes for different choice attributes in decisions motivated by curiosity. *Neuron* **85**, 602–614 (2015).
33. Bromberg-Martin, E. S. & Hikosaka, O. Midbrain dopamine neurons signal preference for advance information about upcoming rewards. *Neuron* **63**, 119–126 (2009).
34. Park, I. M., Meister, M. L., Huk, A. C. & Pillow, J. W. Encoding and decoding in parietal cortex during sensorimotor decision making. *Nat. Neurosci.* **10**, 1395–1403 (2014).
35. Hikosaka, O. & Isoda, M. Switching from automatic to controlled behavior: cortico-basal ganglia mechanisms. *Trends Cogn. Sci.* **14**, 154–161 (2010).
36. Isoda, M. & Hikosaka, O. A neural correlate of motivational conflict in the superior colliculus of the macaque. *J. Neurophysiol.* **100**, 1332–1342 (2008).
37. Leathers, M. L. & Olson, C. R. In monkeys making value-based decisions, LIP neurons encode cue salience and not action value. *Science* **338**, 132–135 (2012).
38. Gottlieb, J. & Goldberg, M. E. Activity of neurons in the lateral intraparietal area of the monkey during an antisaccade task. *Nat. Neurosci.* **2**, 906–912 (1999).
39. Snyder, L. H., Batista, A. P. & Andersen, R. A. Change in motor plan, without a change in the spatial locus of attention, modulates activity in posterior parietal cortex. *J. Neurophysiol.* **79**, 2814–2819 (1998).
40. Hosokawa, T., Kennerley, S. W., Sloan, J. & Wallis, J. D. Single-neuron mechanisms underlying cost–benefit analysis in frontal cortex. *J. Neurosci.* **33**, 17385–17397 (2013).

Acknowledgements

The work was supported by NIH grants R24 EY015634 and RO1EY25965 to J.G., and by fellowships from the Danish Council For Independent Research, the Reinholdt W. Jorck og Hustrus Fond and the Marie og MB Richters Fond to M.H.

Author contributions

J.G., N.D. and M.H. designed and implemented the experiment. M.H. and N.D. collected the data. M.H. analyzed the data. J.G. and M.H. wrote the paper.

Competing interests

The authors declare no competing interests.

Additional information

Supplementary information is available for this paper at https://doi.org/10.1038/s41593-019-0440-1.

Reprints and permissions information is available at www.nature.com/reprints.

Correspondence and requests for materials should be addressed to J.G.

Peer review information: *Nature Neuroscience* thanks Jochen Ditterich and the other, anonymous, reviewer(s) for their contribution to the peer review of this work.

Publisher's note: Springer Nature remains neutral with regard to jurisdictional claims in published maps and institutional affiliations.

Methods

General. Data were collected from two adult male rhesus monkeys using standard behavioral and neurophysiological techniques[41]. All methods were approved by the Animal Care and Use Committees of Columbia University and the New York State Psychiatric Institute as complying with the guidelines within the Public Health Service Guide for the Care and Use of Laboratory Animals. Behavioral control was implemented in MonkeyLogic[42], stimuli were presented on a Mitsubishi Diamond Pro 2070 monitor (30.4 × 40.6 cm viewing area), eye tracking was performed using an Applied Science Laboratories model 5000 (digitized at 240 Hz) and action potentials were recorded using an APM digital processing module (Fred Haer). Individual electrodes (glass-coated tungsten electrodes, Alpha Omega, impedance at 1 kHz: 0.5–1 MΩ) were inserted in daily sessions and aimed to the lateral bank of the intraparietal sulcus based on stereotactic coordinates and structural magnetic resonance imaging.

MGS task. After obtaining a well-isolated waveform, a neuron was first screened with a standard MGS task in which a peripheral target was flashed for 300 ms while the monkeys maintained central fixation and, after a 500-ms delay period, the monkeys were rewarded for making a saccade to the remembered target location. Neurons were further tested only if they had spatially tuned visual and delay period responses on this task (Supplementary Fig. 6). For these cells, the RF was mapped by conducting the MGS at four locations, including the estimated RF center and three equally eccentric locations spaced at 90° intervals.

Information-sampling task. Each trial began with the presentation of a fixation point, whose color (red or blue) signaled the RS, and which was initially surrounded by a shape (circle or square) signaling the block type (INF or unINF). When the monkeys fixated this point for a variable period of 1,300–1,500 ms, the circle or square was removed, and the monkeys were shown a display containing a cue (a collection of ~60 dots randomly positioned within a circular aperture with a diameter of 4.6° of visual angle (DVA)) and two targets (white squares measuring 1 × 1 DVA). In the standard geometry, the display was adjusted so that the cue was at the center of the RF of the recorded neuron while the targets were at a 90° angular separation at an equal eccentricity (with all three locations having been tested in the MGS task; Fig. 1a and Supplementary Fig. 2a). After an additional 500 ms delay period, the fixation point was removed, and the monkeys had to make a first saccade to the dots within 50–2,000 ms of the fixation point offset. If the monkeys fixated on the cue for 100 ms, the dots began to move with 100% coherence at a speed of 3.7 DVA s^{-1} toward one of the targets. A trial was scored as correct if the monkeys made a second saccade to the cued target within 0–1,000 ms after motion onset and maintained fixation in a 3° window surrounding this target for an additional 200 ms. The motion was terminated as soon as the eye of the monkey exited the cue window. Correct trials were signaled by an auditory cue (frequency of 500 Hz and duration of 400 ms) and the delivery of a small or large juice reward according to the fixation point color. RSs were, respectively, 300 and 100 ms solenoid open times, that is, a 3:1 magnitude ratio in both monkeys. An error occurring at any point in the trial was followed by no reward and the immediate removal of the visual stimuli.

Each neuron was tested with a minimum of 2 INF blocks and 2 unINF blocks of 50 correct trials each. The blocks were presented in alternating order (Fig. 1b), such that the condition that was presented first (INF or unINF) and the target that was rewarded in the first unINF block was randomized across sessions. In each block, trials were randomly assigned to deliver a small or large reward with 50% probability. In addition, 8% of trials in each block were catch trials, which were identical to the main trials in all respects except that there was no dot motion (the dots remained stationary). The monkeys therefore had to guess the direction of the correct final saccade and were rewarded for making the second saccade to the blocked target in the unINF blocks and to the randomly selected, but not signaled target, in the INF blocks. If the monkeys prematurely broke fixation or had a saccade latency that was outside the allowed window, the trial was scored as incomplete and was immediately repeated with the same RS and motion direction until correctly completed (up to a limit of ten consecutive errors). Trials with erroneous decisions (in which the monkeys made a second saccade with the correct timing but to the wrong target) were not repeated and counted as completed error trials.

To signal which target location was correct in an unINF block, the first ten trials of each unINF block were 'instruction' trials in which the rewarded target had a higher luminance than the unrewarded one (these trials were not included in the data analysis). These signals, together with the extensive practice of the monkeys, resulted in very fast behavioral transitions, as shown by the fact that decision accuracy and VT values changed little as a function of time in a block and differed significantly between the INF and unINF contexts from the very first trial in a block.

After obtaining a dataset with the main geometry in the two-step task, cells were further tested in three control conditions that were presented in randomized order until isolation was lost or the monkeys stopped working. Two conditions presented the two-step task in the same format as described above, but using modified geometries in which a target was in the RF during the delay period before the first saccade (geometry 1) or during the preparation of the second saccade (geometry 2; Supplementary Fig. 2).

In addition, to test for reward sensitivity, neurons were tested in a control one-step saccade task in which the monkeys made a single saccade to a target to obtain a large or small reward. In these trials, the monkeys achieved fixation and, when the fixation point disappeared, made a saccade to a target whose shape (an upward- or downward-pointing triangle) signaled the RS. RSs were identical to those used in the main task. The task randomly interleaved free-choice trials in which the monkeys were offered both reward alternatives (with the large-reward and small-reward targets falling randomly inside or opposite the RF) and forced-choice trials in which a single target was present (either inside or opposite the RF). During the free-choice trials, the monkeys nearly always chose the large RS, which shows that they were highly sensitive to these differences in RS (97.6% in monkey M, 97.8% in monkey S). Neural responses were analyzed on interleaved forced-choice trials, in which we could obtain RF-directed saccades at both reward magnitudes. Note that this task was designed to act as a screening tool for the presence of reward modulations. Therefore, it was designed to emulate the structures of tasks used in previous investigations of reward in this area (for example, see ref. [43]) rather than to provide a systematic comparison with the information-sampling task.

Data analyses. Data are reported from 87 neurons recorded from two 16-year-old male monkeys (49 neurons in monkey M, 38 neurons in monkey S) that were tested in the standard geometry of the two-step task. Of these cells, 36 neurons were further tested in control geometry 1 (26 in monkey M), 48 neurons (30 in monkey M) were tested in geometry 2, and 56 neurons (36 in monkey M) were tested with the one-step reward control task. No statistical methods were used to predetermine sample sizes, but our sample sizes were similar to those reported in previous studies of this area[8,14,37]. Data collection and analyses were not performed blinded to the conditions of the experiments. Error trials were not considered in the analysis of neural responses. All statistical comparisons used nonparametric tests (two-sided paired rank or signed-rank tests) unless otherwise noted. The Nature Research Reporting Summary contains summaries of statistics and data of this Methods section.

The 'trial completion' rate (Fig. 2) was the number of completed trials divided by the number of the trials in which the monkeys initiated fixation. The 'decision accuracy' was the number of rewarded trials divided by the number of completed trials. Beyond the analysis of completion rates, incomplete trials were discarded and not further analyzed. The saccade latency was measured between the fixation point offset and the saccade start, as defined based on velocity and acceleration criteria[44]. The 'endpoint accuracy' was defined as the Euclidean distance between the center of the cue/target and the saccade landing position, the 'velocity' refers to the peak saccade velocity, and the VT was the interval between the motion onset and the start of the second saccade. Note that because the monkeys had to complete 100 ms of post-saccadic fixation before motion onset, the inter-saccadic interval (that is, the latency of the second saccade) was equal to VT + 100 ms.

Delay-period FRs were measured from the raw spike trains.

For each neuron, trial-by-trial FRs were fit with two regression equations as follows:

$$\begin{aligned} FR = {} & \beta_0 + \beta_{IG} \times IG + \beta_{RS} \times RS + \beta_{LAT} \times RT \\ & + \beta_{VEL} \times VEL + \beta_{ACC} \times ACC \\ & + \beta_{VT} \times VT + \beta_{SDIR} \times SDIR \end{aligned} \quad (1)$$

$$\begin{aligned} FR = {} & \beta_0 + \beta_{IG} \times IG + \beta_{RS} \times RS + \beta_{INT} \\ & \times IG \times RS + \beta_{LAT} \times RT + \beta_{VEL} \times VEL \\ & + \beta_{ACC} \times ACC + \beta_{VT} \times VT + \beta_{SDIR} \times SDIR \end{aligned} \quad (2)$$

IG is the information gain (0 for unINF, 1 for INF) and RS is the reward size (0 for small, 1 for large). The coefficients for LAT, VEL ACC capture the effects of, respectively, the RT, velocity and accuracy of the first saccade. VT is the motion viewing time and SDIR is the direction of the second saccade. SDIR was arbitrarily set to 0 or 1 for each of the two final saccades. The fits were implemented with the stepwiselm function in MATLAB v.2014b. All the regressors were *z*-scored using all the trials in a session. The IG and RS terms in equation (1), and the IG, RS and IG–RS terms in equation (2) were locked in the model. The remaining saccade descriptors were included according to a backward stepwise procedure using *P* values of 0.05 and 0.10 as cut-offs for, respectively, including and excluding regressors[14].

All analyses were done on raw FRs and repeated with *z*-scored and mean-normalized FRs. Unless otherwise noted, regression coefficients are reported in units of sp s^{-1}. Exploratory analyses showed that the IG and RS effects were sustained during the delay period (Fig. 3b; Supplementary Fig. 3c) and were not sensitive to a range of window sizes spanning this period. Thus, the results are based on the FR averaged throughout the delay period (that is, 150 ms after cue onset until the saccade onset).

The TRF measured the extent to which the targets encroached on the RF of a cell in the standard geometry of the two-step task. The TRF was computed for each cell as follows:

$$TRF = \frac{FR_{cue\_loc} - FR_{tar\_loc}}{FR_{cue\_loc} + FR_{tar\_loc}} \quad (3)$$

All FR values were measured during the delay period of the MGS task (300–800 ms after cue onset). FR_{cue_loc} is the FR at the RF center (the location occupied by the cue in the standard geometry of the two-step task), FR_{tar_loc} is the average FR at the two locations closest to the center (the same locations that were occupied by the targets in the standard geometry of the two-step task). The TRF ranges between 1 (indicating a cell that does not respond at all at the target locations) and 0 (indicating a cell that responded equivalently to the cue and target locations). Note that negative values are impossible in this index since the cue location had been pre-selected as the location that had a higher FR.

Reporting Summary. Further information on research design is available in the Nature Research Reporting Summary linked to this article.

Data availability

The data generated and analyzed for this study are available from the corresponding author upon request.

Code availability

The code written to analyze the data and to produce the figures for this study are available from the corresponding author upon request.

References

41. Oristaglio, J., Schneider, D. M., Balan, P. F. & Gottlieb, J. Integration of visuospatial and effector information during symbolically cued limb movements in monkey lateral intraparietal area. *J. Neurosci.* **26**, 8310–8319 (2006).
42. Asaad, W. F. & Eskandar, E. N. A flexible software tool for temporally-precise behavioral control in Matlab. *J. Neurosci. Methods* **174**, 245–258 (2008).
43. Platt, M. L. & Glimcher, P. W. Neural correlates of decision variables in parietal cortex. *Nature* **400**, 233–238 (1999).
44. Nystrom, M. & Holmqvist, K. An adaptive algorithm for fixation, saccade, and glissade detection in eyetracking data. *Behav. Res. Methods* **42**, 188–204 (2010).

nature research

Corresponding author(s): Jacqueline Gottlieb

Last updated by author(s): May 15, 2019

Reporting Summary

Nature Research wishes to improve the reproducibility of the work that we publish. This form provides structure for consistency and transparency in reporting. For further information on Nature Research policies, see Authors & Referees and the Editorial Policy Checklist.

Statistics

For all statistical analyses, confirm that the following items are present in the figure legend, table legend, main text, or Methods section.

n/a	Confirmed	
☐	☒	The exact sample size (*n*) for each experimental group/condition, given as a discrete number and unit of measurement
☐	☒	A statement on whether measurements were taken from distinct samples or whether the same sample was measured repeatedly
☐	☒	The statistical test(s) used AND whether they are one- or two-sided *Only common tests should be described solely by name; describe more complex techniques in the Methods section.*
☐	☒	A description of all covariates tested
☐	☒	A description of any assumptions or corrections, such as tests of normality and adjustment for multiple comparisons
☐	☒	A full description of the statistical parameters including central tendency (e.g. means) or other basic estimates (e.g. regression coefficient) AND variation (e.g. standard deviation) or associated estimates of uncertainty (e.g. confidence intervals)
☐	☒	For null hypothesis testing, the test statistic (e.g. *F*, *t*, *r*) with confidence intervals, effect sizes, degrees of freedom and *P* value noted *Give P values as exact values whenever suitable.*
☒	☐	For Bayesian analysis, information on the choice of priors and Markov chain Monte Carlo settings
☒	☐	For hierarchical and complex designs, identification of the appropriate level for tests and full reporting of outcomes
☐	☒	Estimates of effect sizes (e.g. Cohen's *d*, Pearson's *r*), indicating how they were calculated

Our web collection on statistics for biologists contains articles on many of the points above.

Software and code

Policy information about availability of computer code

Data collection	Monkeylogic, September 2012 edition
Data analysis	MATLAB R2014b, used to write custom code

For manuscripts utilizing custom algorithms or software that are central to the research but not yet described in published literature, software must be made available to editors/reviewers. We strongly encourage code deposition in a community repository (e.g. GitHub). See the Nature Research guidelines for submitting code & software for further information.

Data

Policy information about availability of data

All manuscripts must include a data availability statement. This statement should provide the following information, where applicable:

- Accession codes, unique identifiers, or web links for publicly available datasets
- A list of figures that have associated raw data
- A description of any restrictions on data availability

The data generated and analyzed for this study are available from the corresponding author upon request.

Field-specific reporting

Please select the one below that is the best fit for your research. If you are not sure, read the appropriate sections before making your selection.

☒ Life sciences ☐ Behavioural & social sciences ☐ Ecological, evolutionary & environmental sciences

For a reference copy of the document with all sections, see nature.com/documents/nr-reporting-summary-flat.pdf

Life sciences study design

All studies must disclose on these points even when the disclosure is negative.

Sample size	Two animal subjects with a total of 87 neurons. Based on the literature, this is an average sample size for the effects we expected in LIP. No statistical methods were used to pre-determine sample sizes.
Data exclusions	Neurons were selected based on pre-defined, standard, electrophysiological response patterns, as outlined in manuscript. Error trials were not considered in analysis of neural responses. This exclusion was pre-established to focus on trials of interest.
Replication	Results were replicated in two animals and in 87 independently sampled cells.
Randomization	The process of selecting the neurons is a random sample of LIP on a given experimental session. Experimental conditions were randomized within and across sessions.
Blinding	Investigators were not blinded. Blinding is irrelevant, because the results are based on statistical analyses, the exclusion criteria are separate from the phenomena being investigated, clearly reported, and standard in the field.

Behavioural & social sciences study design

All studies must disclose on these points even when the disclosure is negative.

Study description	*Briefly describe the study type including whether data are quantitative, qualitative, or mixed-methods (e.g. qualitative cross-sectional, quantitative experimental, mixed-methods case study).*
Research sample	*State the research sample (e.g. Harvard university undergraduates, villagers in rural India) and provide relevant demographic information (e.g. age, sex) and indicate whether the sample is representative. Provide a rationale for the study sample chosen. For studies involving existing datasets, please describe the dataset and source.*
Sampling strategy	*Describe the sampling procedure (e.g. random, snowball, stratified, convenience). Describe the statistical methods that were used to predetermine sample size OR if no sample-size calculation was performed, describe how sample sizes were chosen and provide a rationale for why these sample sizes are sufficient. For qualitative data, please indicate whether data saturation was considered, and what criteria were used to decide that no further sampling was needed.*
Data collection	*Provide details about the data collection procedure, including the instruments or devices used to record the data (e.g. pen and paper, computer, eye tracker, video or audio equipment) whether anyone was present besides the participant(s) and the researcher, and whether the researcher was blind to experimental condition and/or the study hypothesis during data collection.*
Timing	*Indicate the start and stop dates of data collection. If there is a gap between collection periods, state the dates for each sample cohort.*
Data exclusions	*If no data were excluded from the analyses, state so OR if data were excluded, provide the exact number of exclusions and the rationale behind them, indicating whether exclusion criteria were pre-established.*
Non-participation	*State how many participants dropped out/declined participation and the reason(s) given OR provide response rate OR state that no participants dropped out/declined participation.*
Randomization	*If participants were not allocated into experimental groups, state so OR describe how participants were allocated to groups, and if allocation was not random, describe how covariates were controlled.*

Ecological, evolutionary & environmental sciences study design

All studies must disclose on these points even when the disclosure is negative.

Study description	*Briefly describe the study. For quantitative data include treatment factors and interactions, design structure (e.g. factorial, nested, hierarchical), nature and number of experimental units and replicates.*
Research sample	*Describe the research sample (e.g. a group of tagged Passer domesticus, all Stenocereus thurberi within Organ Pipe Cactus National Monument), and provide a rationale for the sample choice. When relevant, describe the organism taxa, source, sex, age range and any manipulations. State what population the sample is meant to represent when applicable. For studies involving existing datasets, describe the data and its source.*
Sampling strategy	*Note the sampling procedure. Describe the statistical methods that were used to predetermine sample size OR if no sample-size calculation was performed, describe how sample sizes were chosen and provide a rationale for why these sample sizes are sufficient.*
Data collection	*Describe the data collection procedure, including who recorded the data and how.*
Timing and spatial scale	*Indicate the start and stop dates of data collection, noting the frequency and periodicity of sampling and providing a rationale for*

Timing and spatial scale	*these choices. If there is a gap between collection periods, state the dates for each sample cohort. Specify the spatial scale from which the data are taken*
Data exclusions	*If no data were excluded from the analyses, state so OR if data were excluded, describe the exclusions and the rationale behind them, indicating whether exclusion criteria were pre-established.*
Reproducibility	*Describe the measures taken to verify the reproducibility of experimental findings. For each experiment, note whether any attempts to repeat the experiment failed OR state that all attempts to repeat the experiment were successful.*
Randomization	*Describe how samples/organisms/participants were allocated into groups. If allocation was not random, describe how covariates were controlled. If this is not relevant to your study, explain why.*
Blinding	*Describe the extent of blinding used during data acquisition and analysis. If blinding was not possible, describe why OR explain why blinding was not relevant to your study.*

Did the study involve field work? ☐ Yes ☐ No

Field work, collection and transport

Field conditions	*Describe the study conditions for field work, providing relevant parameters (e.g. temperature, rainfall).*
Location	*State the location of the sampling or experiment, providing relevant parameters (e.g. latitude and longitude, elevation, water depth).*
Access and import/export	*Describe the efforts you have made to access habitats and to collect and import/export your samples in a responsible manner and in compliance with local, national and international laws, noting any permits that were obtained (give the name of the issuing authority, the date of issue, and any identifying information).*
Disturbance	*Describe any disturbance caused by the study and how it was minimized.*

Reporting for specific materials, systems and methods

We require information from authors about some types of materials, experimental systems and methods used in many studies. Here, indicate whether each material, system or method listed is relevant to your study. If you are not sure if a list item applies to your research, read the appropriate section before selecting a response.

Materials & experimental systems

n/a	Involved in the study
☒	☐ Antibodies
☒	☐ Eukaryotic cell lines
☒	☐ Palaeontology
☐	☒ Animals and other organisms
☒	☐ Human research participants
☒	☐ Clinical data

Methods

n/a	Involved in the study
☒	☐ ChIP-seq
☒	☐ Flow cytometry
☒	☐ MRI-based neuroimaging

Antibodies

Antibodies used	*Describe all antibodies used in the study; as applicable, provide supplier name, catalog number, clone name, and lot number.*
Validation	*Describe the validation of each primary antibody for the species and application, noting any validation statements on the manufacturer's website, relevant citations, antibody profiles in online databases, or data provided in the manuscript.*

Eukaryotic cell lines

Policy information about cell lines

Cell line source(s)	*State the source of each cell line used.*
Authentication	*Describe the authentication procedures for each cell line used OR declare that none of the cell lines used were authenticated.*
Mycoplasma contamination	*Confirm that all cell lines tested negative for mycoplasma contamination OR describe the results of the testing for mycoplasma contamination OR declare that the cell lines were not tested for mycoplasma contamination.*
Commonly misidentified lines (See ICLAC register)	*Name any commonly misidentified cell lines used in the study and provide a rationale for their use.*

Palaeontology

Specimen provenance	*Provide provenance information for specimens and describe permits that were obtained for the work (including the name of the issuing authority, the date of issue, and any identifying information).*
Specimen deposition	*Indicate where the specimens have been deposited to permit free access by other researchers.*
Dating methods	*If new dates are provided, describe how they were obtained (e.g. collection, storage, sample pretreatment and measurement), where they were obtained (i.e. lab name), the calibration program and the protocol for quality assurance OR state that no new dates are provided.*

☐ Tick this box to confirm that the raw and calibrated dates are available in the paper or in Supplementary Information.

Animals and other organisms

Policy information about studies involving animals; ARRIVE guidelines recommended for reporting animal research

Laboratory animals	2 Rhesus monkeys (macaca mulatta), male, adult, age 16
Wild animals	Wild animals were not used in this study.
Field-collected samples	Field samples were not used in this study.
Ethics oversight	All methods were approved by the Animal Care and Use Committees of Columbia University and New York State Psychiatric Institute as complying with the guidelines within the Public Health Service Guide for the Care and Use of Laboratory Animals.

Note that full information on the approval of the study protocol must also be provided in the manuscript.

Human research participants

Policy information about studies involving human research participants

Population characteristics	*Describe the covariate-relevant population characteristics of the human research participants (e.g. age, gender, genotypic information, past and current diagnosis and treatment categories). If you filled out the behavioural & social sciences study design questions and have nothing to add here, write "See above."*
Recruitment	*Describe how participants were recruited. Outline any potential self-selection bias or other biases that may be present and how these are likely to impact results.*
Ethics oversight	*Identify the organization(s) that approved the study protocol.*

Note that full information on the approval of the study protocol must also be provided in the manuscript.

Clinical data

Policy information about clinical studies

All manuscripts should comply with the ICMJE guidelines for publication of clinical research and a completed CONSORT checklist must be included with all submissions.

Clinical trial registration	*Provide the trial registration number from ClinicalTrials.gov or an equivalent agency.*
Study protocol	*Note where the full trial protocol can be accessed OR if not available, explain why.*
Data collection	*Describe the settings and locales of data collection, noting the time periods of recruitment and data collection.*
Outcomes	*Describe how you pre-defined primary and secondary outcome measures and how you assessed these measures.*

ChIP-seq

Data deposition

☐ Confirm that both raw and final processed data have been deposited in a public database such as GEO.

☐ Confirm that you have deposited or provided access to graph files (e.g. BED files) for the called peaks.

Data access links *May remain private before publication.*	*For "Initial submission" or "Revised version" documents, provide reviewer access links. For your "Final submission" document, provide a link to the deposited data.*
Files in database submission	*Provide a list of all files available in the database submission.*

Genome browser session
(e.g. UCSC)

Provide a link to an anonymized genome browser session for "Initial submission" and "Revised version" documents only, to enable peer review. Write "no longer applicable" for "Final submission" documents.

Methodology

Replicates

Describe the experimental replicates, specifying number, type and replicate agreement.

Sequencing depth

Describe the sequencing depth for each experiment, providing the total number of reads, uniquely mapped reads, length of reads and whether they were paired- or single-end.

Antibodies

Describe the antibodies used for the ChIP-seq experiments; as applicable, provide supplier name, catalog number, clone name, and lot number.

Peak calling parameters

Specify the command line program and parameters used for read mapping and peak calling, including the ChIP, control and index files used.

Data quality

Describe the methods used to ensure data quality in full detail, including how many peaks are at FDR 5% and above 5-fold enrichment.

Software

Describe the software used to collect and analyze the ChIP-seq data. For custom code that has been deposited into a community repository, provide accession details.

Flow Cytometry

Plots

Confirm that:

☐ The axis labels state the marker and fluorochrome used (e.g. CD4-FITC).

☐ The axis scales are clearly visible. Include numbers along axes only for bottom left plot of group (a 'group' is an analysis of identical markers).

☐ All plots are contour plots with outliers or pseudocolor plots.

☐ A numerical value for number of cells or percentage (with statistics) is provided.

Methodology

Sample preparation

Describe the sample preparation, detailing the biological source of the cells and any tissue processing steps used.

Instrument

Identify the instrument used for data collection, specifying make and model number.

Software

Describe the software used to collect and analyze the flow cytometry data. For custom code that has been deposited into a community repository, provide accession details.

Cell population abundance

Describe the abundance of the relevant cell populations within post-sort fractions, providing details on the purity of the samples and how it was determined.

Gating strategy

Describe the gating strategy used for all relevant experiments, specifying the preliminary FSC/SSC gates of the starting cell population, indicating where boundaries between "positive" and "negative" staining cell populations are defined.

☐ Tick this box to confirm that a figure exemplifying the gating strategy is provided in the Supplementary Information.

Magnetic resonance imaging

Experimental design

Design type

Indicate task or resting state; event-related or block design.

Design specifications

Specify the number of blocks, trials or experimental units per session and/or subject, and specify the length of each trial or block (if trials are blocked) and interval between trials.

Behavioral performance measures

State number and/or type of variables recorded (e.g. correct button press, response time) and what statistics were used to establish that the subjects were performing the task as expected (e.g. mean, range, and/or standard deviation across subjects).

Acquisition

Imaging type(s) — *Specify: functional, structural, diffusion, perfusion.*

Field strength — *Specify in Tesla*

Sequence & imaging parameters — *Specify the pulse sequence type (gradient echo, spin echo, etc.), imaging type (EPI, spiral, etc.), field of view, matrix size, slice thickness, orientation and TE/TR/flip angle.*

Area of acquisition — *State whether a whole brain scan was used OR define the area of acquisition, describing how the region was determined.*

Diffusion MRI ☐ Used ☐ Not used

Preprocessing

Preprocessing software — *Provide detail on software version and revision number and on specific parameters (model/functions, brain extraction, segmentation, smoothing kernel size, etc.).*

Normalization — *If data were normalized/standardized, describe the approach(es): specify linear or non-linear and define image types used for transformation OR indicate that data were not normalized and explain rationale for lack of normalization.*

Normalization template — *Describe the template used for normalization/transformation, specifying subject space or group standardized space (e.g. original Talairach, MNI305, ICBM152) OR indicate that the data were not normalized.*

Noise and artifact removal — *Describe your procedure(s) for artifact and structured noise removal, specifying motion parameters, tissue signals and physiological signals (heart rate, respiration).*

Volume censoring — *Define your software and/or method and criteria for volume censoring, and state the extent of such censoring.*

Statistical modeling & inference

Model type and settings — *Specify type (mass univariate, multivariate, RSA, predictive, etc.) and describe essential details of the model at the first and second levels (e.g. fixed, random or mixed effects; drift or auto-correlation).*

Effect(s) tested — *Define precise effect in terms of the task or stimulus conditions instead of psychological concepts and indicate whether ANOVA or factorial designs were used.*

Specify type of analysis: ☐ Whole brain ☐ ROI-based ☐ Both

Statistic type for inference (See Eklund et al. 2016) — *Specify voxel-wise or cluster-wise and report all relevant parameters for cluster-wise methods.*

Correction — *Describe the type of correction and how it is obtained for multiple comparisons (e.g. FWE, FDR, permutation or Monte Carlo).*

Models & analysis

n/a	Involved in the study
☐	☐ Functional and/or effective connectivity
☐	☐ Graph analysis
☐	☐ Multivariate modeling or predictive analysis

Functional and/or effective connectivity — *Report the measures of dependence used and the model details (e.g. Pearson correlation, partial correlation, mutual information).*

Graph analysis — *Report the dependent variable and connectivity measure, specifying weighted graph or binarized graph, subject- or group-level, and the global and/or node summaries used (e.g. clustering coefficient, efficiency, etc.).*

Multivariate modeling and predictive analysis — *Specify independent variables, features extraction and dimension reduction, model, training and evaluation metrics.*